Critical Care

RESEARCH

Open Access

Atelectrauma can be avoided if expiration is sufficiently brief: evidence from inverse modeling and oscillometry during airway pressure release ventilation

Jason H. T. Bates[1*], David W. Kaczka[2], Michaela Kollisch-Singule[3], Gary F. Nieman[3] and Donald P. Gaver[4]

Abstract

Background Airway pressure release ventilation (APRV) has been shown to be protective against atelectrauma if expirations are brief. We hypothesize that this is protective because epithelial surfaces are not given enough time to come together and adhere during expiration, thereby avoiding their highly damaging forced separation during inspiration.

Methods We investigated this hypothesis in a porcine model of ARDS induced by Tween lavage. Animals were ventilated with APRV in 4 groups based on whether inspiratory pressure was 28 or 40 cmH_2O, and whether expiration was terminated when end-expiratory flow reached either 75% (a shorter expiration) or 25% (a longer expiration) of its initial peak value. A mathematical model of respiratory system mechanics that included a volume-dependent elastance term characterized by the parameter E_2 was fit to airway pressure-flow data obtained each hour for 6 h post-Tween injury during both expiration and inspiration. We also measured respiratory system impedance between 5 and 19 Hz continuously through inspiration at the same time points from which we derived a time-course for respiratory system resistance (R_{rs}).

Results E_2during both expiration and inspiration was significantly different between the two longer expiration versus the two shorter expiration groups (ANOVA, $p < 0.001$). We found that E_2 was most depressed during inspiration in the higher-pressure group receiving the longer expiration, suggesting that E_2 reflects a balance between strain stiffening of the lung parenchyma and ongoing recruitment as lung volume increases. We also found in this group that R_{rs} increased progressively during the first 0.5 s of inspiration and then began to decrease again as inspiration continued, which we interpret as corresponding to the point when continuing derecruitment was reversed by progressive lung inflation.

Conclusions These findings support the hypothesis that sufficiently short expiratory durations protect against atelectrauma because they do not give derecruitment enough time to manifest. This suggests a means for the personalized adjustment of mechanical ventilation.

Keywords Ventilator-induced lung injury, Porcine lavage model, Mathematical model, Respiratory system impedance, Over-distension

*Correspondence:
Jason H. T. Bates
jason.h.bates@uvm.edu
Full list of author information is available at the end of the article

Background

Ventilator-induced lung injury (VILI) is a common and potentially fatal complication in mechanically ventilated patients with acute respiratory distress syndrome (ARDS). Applying mechanical ventilation in a way that reduces the chances of incurring VILI is thus a high priority in these patients, especially since VILI becomes increasingly difficult to reverse once it is underway [1, 2]. A key pathway to VILI is atelectrauma, which results from cyclic inspiratory re-opening of lung units that close during expiration [3–5]. One perceived management strategy for avoiding atelectrauma is the application of an "appropriate" level of positive end-expiratory pressure (PEEP) [6]. The rationale for this strategy is that derecruitment is a phenomenon that depends on transpulmonary pressure [7], so limiting lung deflation limits derecruitment accordingly. Nevertheless, deciding on the precise level of PEEP for a given patient has proven problematic [8]. Indeed, although PEEP is universally used when ventilating injured lungs and has been shown to improve oxygenation and reduce lung compliance, no PEEP selection strategy has been shown to reduce mortality [9–11].

Derecruitment does not depend solely on lung inflation pressure, however. It is also a function of time [12, 13], which means that closure of lung units can be manipulated by adjustments in expiratory duration, in addition to PEEP. Indeed, reduction in atelectrauma has been demonstrated using airway pressure release ventilation (APRV) employed with very brief expirations [4, 14, 15]. Specifically, experimental animal studies have shown lung-protective benefits of APRV when expiration is terminated at the point where end-expiratory flow (EEF) has fallen to 75% of its initial peak value [4, 16]. This results in an expiratory duration of about 0.5 s, which is much shorter than in conventional ventilation but still sufficient for adequate CO_2 elimination. Alternatively, allowing EEF to fall to 25% of its peak value can yield an expiratory duration in the order of 1.0–1.5 s, and results in evidence of VILI [17]. We previously hypothesized that such findings are due to the fact that recruitment and derecruitment of lung tissue depend on time as well as pressure [18]. That is, alveoli and small airways require a certain amount of time to collapse or become occluded during expiration, independent of the applied airway pressure. Consequently, a sufficiently brief expiration does not allow enough time for epithelial surfaces to come into apposition and adhere to each other as lung volume decreases, thereby avoiding their highly stressful forced separation during inspiration.

While a case might be made for the plausibility of this hypothesis, there remains little direct evidence to support it. Furthermore, the choice of expiratory duration based on EEF is purely empirical, and it remains unclear whether termination of EEF at 75% of its peak value is in fact "optimal". Clarifying such issues could have important implications for protective ventilation of patients with ARDS. In this study, we addressed these issues by measuring lung function throughout the APRV breath in a porcine model of acute lung injury. We used indices of respiratory resistive and elastic properties as indicators of the presence of lung overdistention and derecruitment.

Methods

Data for this study were collected during porcine experiments described previously [4, 17]. The protocol was approved by the Institutional Animal Care and Use Committee at the State University of New York Upstate Medical University, in accordance with the ARRIVE guidelines [19]. Relevant aspects of these experiments are summarized below and involve very different data analyses as well as collection of additional data not described previously. The investigators involved in conducting the experiments were not blinded to treatment groups.

Surgical preparation

Female Yorkshire pigs (38.3 ± 1.8 kg, ~ 6 months of age) were anesthetized (ketamine 9 mg/1 mL + xylazine 0.009 mg/1 mL at 1 mg/kg/hr continuous i.v. infusion, titrated to maintain a Stage III surgical plane of anesthesia), and mechanically ventilated (Dräger Evita Infinity V500) via a 7.5-mm endotracheal tube (Hudson RCI, Teleflex Medical, Research Triangle Park, NC) placed into a tracheotomy. Central venous catheters were placed into the bilateral external jugular veins for administration of fluids and medications. The animals were initially ventilated with a tidal volume (Vt) of 10 mL/kg, a respiratory rate (RR) of 12 breaths/min, a PEEP of 5 cmH_2O, and a fraction of inspired oxygen (FiO_2) of 1.0.

Initiation of acute lung injury

A bronchoscope was advanced into the right mainstem bronchus, past the right middle lobe bronchus, during 20 cm H_2O continuous positive airway pressure [4, 17]. A 3% Tween-20 detergent solution (0.75 mL/kg) was instilled into the basilar lung regions to deactivate pulmonary surfactant [20]. This procedure was repeated through the left mainstem bronchus and past the left cranial lobe bronchus [4, 17], where another (0.75 mL/kg) Tween dose was administered.

Animals received intravenous resuscitation with Lactated Ringers, with 1L boluses administered to maintain mean arterial pressure (MAP) greater than

65 mmHg. Lack of fluid responsiveness was identified by the requirement for two boluses within 1 h, in which case a norepinephrine (2–20mcg/min) infusion was started and titrated to achieve a MAP > 65 mmHg. Following injury, FiO_2 was titrated to a minimum of 0.3 if oxygenation improved, with a goal peripheral oxygen saturation above 90%.

Mechanical ventilation

After neuromuscular blockade with rocuronium (0.01–0.012 mg/kg/min) to avoid an inspiratory drive reflex, the animals were switched to APRV defined by: 1) the value of the constant airway pressure during inspiration (P_{High}); 2) the duration of inspiration (T_{High}); 3) the ventilator pressure applied during expiration (P_{Low}); and 4) the duration of expiration (T_{Low}). Each pig was then randomized to one of four groups based on the risk (±) for intratidal overdistention (OD) and atelectrauama from recruitment/derecruitment (RD): 1) OD−RD−; 2) OD−RD+; 3) OD+RD-; and 4) OD+RD+. Thus, the two OD- groups received $P_{High} = 28$ cm H_2O per clinical guidelines [21], while the two OD+groups received $P_{High} = 40$ cm H_2O. The two RD- groups had expiration terminated when flow had fallen to 75% of peak, resulting in values of T_{Low} in the order of 0.5 s. The two RD+groups had expiration terminated when flow had fallen to 25% of peak, resulting in $T_{Low} > 1$ s, which has been shown to lead to atelectrauma [22]. PaO_2/FiO_2 ratio was assessed hourly and FiO_2 was titrated to maintain PaO_2:FiO_2 ratio above 300. We have previously shown [4] that the PaO_2:FiO_2 ratio in these groups after 6 h of mechanical ventilation was stratified from worst to best as OD+RD+, OD−RD+, OD+RD−, and OD−RD−. This was an exploratory study for which an informed power analysis is essentially impossible, so our choice of for $n = 10$ per group was arbitrary. This choice is nevertheless supported by a prior study in a similar animal model, with $n = 10$ per group to achieve alpha = 0.05 and power = 90% [17]. Dropouts due to technical issues resulted in $n = 10$ for OD-RD-, $n = 7$ for OD-RD+, $n = 9$ for OD+RD- and $n = 9$ for OD+RD+.

Collection of airway pressure and flow signals

Airflow at the proximal end of the endotracheal tube was measured with a pneumotachograph (Hans Rudolph, 3700 Series 0–160 L/min). A differential piezoresistive pressure sensor measured the pressure drop across the pneumotachograph to determine flow ($\dot{V}$), while a gauge pressure sensor measured airway opening pressure (P) (SC-24, Scireq, Montreal). The $\dot{V}$ and P signals were low-pass filtered at 30 Hz (SC-24, Scireq, Montreal) and sampled at 256 Hz with a 16-bit analog-to-digital converter (NI USB-6212 (BNC) DAQ, National Instruments, Austin, TX) using Labview™ (National Instruments, TX). Ten-second epochs of data were collected under two conditions: 1) during mechanical ventilation only for the purposes of fitting time-domain models of respiratory system mechanics (see below); and 2) during mechanical ventilation combined with the application of broad-band high-frequency flow oscillations for the purposes of determining respiratory system impedance (see below). Each pair of 10-s epochs of $\dot{V}$ and P recorded during either condition contained approximately two complete mechanically ventilated breaths. The data from the two conditions were analyzed as follows.

Time-domain model fitting

$\dot{V}$ Was numerically integrated with respect to time (t) to yield volume (V), which was corrected for drift through the addition of a constant to $\dot{V}$ such that the end-inspiratory peak values of V between the two breaths in each data epoch were equal. The end-expiratory value of V in each recording was designated as $V = 0$. The five models listed in Table 1 were fit by multiple linear regression to segments of the recorded data (see Results) [23]. These models were chosen because they represent a hierarchical approach to representing lung mechanics in increasing order of complexity [23].

Model 1 represents the single-compartment linear model of respiratory system mechanics, with free parameters R, E, λ and P_0. R denotes total respiratory resistance, while E denotes total respiratory elastance. λ absorbs any uncertainty in the correction of volume drift, while P_0 allows for the arbitrary decision

Table 1 The five time-domain models of respiratory system mechanics fit to segments of $\dot{V}(t)$ and $P(t)$

Model designation	Equation of motion
Model 1:	$P(t) = R\dot{V}(t) + EV(t) + \lambda t + P_0$
Model 2:	$P(t) = R_1\dot{V}(t) + R_2\dot{V}(t)\lvert\dot{V}(t)\rvert + EV(t) + \lambda t + P_0$
Model 3:	$P(t) = R\dot{V}(t) + E_1V(t) + E_2V^2(t) + \lambda t + P_0$
Model 4:	$P(t) = R_1\dot{V}(t) + R_2\dot{V}(t)\lvert\dot{V}(t)\rvert + E_1V(t) + E_1V^2(t) + \lambda t + P_0$
Model 5:	$P(t) = \alpha\dot{V} + \beta V(t) + \gamma\int_0^t V(t)dt + \delta\int_0^t P(t)dt + \lambda t + \rho$

as to when $V = 0$. Model 2 represents the single-compartment model having a flow-dependent resistance, with free parameters R_1 and R_2 that denote flow-independent and flow-dependent components of resistance, respectively [24] along with the same parameters E, λ and P_0 from Model 1. Model 3 has the same free parameters R, λ, and P_0 as Model 1, with two additional parameters, E_1 and E_2, to denote volume-independent and volume-dependent elastance, respectively [25–27] Model 4 is the combination of Model 2 and Model 3, with free parameters R_1, R_2, E_1, E_2, λ and P_0. Finally, Model 5 is the generalized two-compartment linear model of respiratory system mechanics, with free parameters α, β, γ, δ, λ and ρ [28]. The definite integrals of $V(t)$ and $P(t)$ in Model 5 were calculated using the first-order Euler method, with $t = 0$ being the start of each data epoch. The relative goodness-of-fit for each model was quantified using the root mean squared residual (RMSR) and the corrected Akaike criterion (AICc). The corresponding Akaike weights specified the likelihoods of each model being the best [29, 30].

Time-course of oscillometric impedance

Oscillometric measurements of respiratory system mechanics were made as described previously [4] using a loudspeaker encased in a rigid enclosure with the front chamber of the enclosure connected to the ventilator circuit near the entrance to the endotracheal tube. The front and back chambers of the enclosure were connected with a tube so that slowly varying circuit pressures due to mechanical ventilation could equilibrate on either side of the speaker cone to prevent it from being driven to the end of its travel during inspiration. The speaker produced a superposition of 6 sinewaves having mutually prime frequencies of 5, 7, 11, 13, 17 and 19 Hz, with peak-to-peak flow amplitudes that were roughly constant over this frequency range. The speaker was activated by a Pyle-PTA-1000 power amplifier driven by a digital signal from Labview™ (National Instruments, TX).

Epochs of forced oscillatory flow were applied to the ventilator circuit. Using custom software, the oscillatory flow and pressure signals were digitally high-pass filtered from the total signals to isolate them from the ventilator waveforms. Respiratory system impedance was calculated at the designated oscillation frequencies as the ratio of the fast Fourier transforms of pressure to flow. This calculation was performed within a 1 s sliding window that moved over the 10-s length of the data in increments of 0.0078 ms. This produced a sequence of impedances at a frequency of 128 Hz.

In order to encapsulate impedance in terms of a small number of parameters, the impedance from each 1-s window was fit with the impedance predicted by a linear single-compartment resistance-elastance-inertance model of the respiratory given by

$$Z(f) = R_{rs} + i\left(2\pi f I_{rs} - \frac{E_{rs}}{2\pi f}\right) \quad (1)$$

where R_{rs} is respiratory system resistance, I_{rs} is respiratory system inertance, E_{rs} is respiratory system elastance, and $i = \sqrt{-1}$ [23].

Note that R_{rs} and E_{rs} are related to the quantities R and E in Model 1 (Table 1) but were obtained from data having very different bandwidths. That is, R and E pertain to the frequency of mechanical ventilation whereas R_{rs}, I_{rs} and E_{rs} pertain to the 5–19 Hz frequency range imposed by oscillometry, so these two sets of parameters reflect somewhat different physiologic information [23]. Also, while model fitting provided single values of R and E for an entire epoch of data, the above frequency-domain analysis provided R_{rs}, I_{rs} and E_{rs} as functions of time.

Measurement protocol

Ten-second epochs of $\dot{V}$ and P both with and without superimposed flow oscillations were collected under baseline conditions at the start of the experimental protocol at the time point designated BL, immediately following Tween instillation at the time point designated T0, and then every subsequent hour for 6 h (time points T1 through T6). Out of a total of 280 instances of data collection without oscillations (8 time points in 35 pigs), technical failures resulted in data being discarded at a single time point in two of the pigs, leaving 278 satisfactory data epochs. In the 280 instances of data collection with flow oscillations, corrupted data at a single time point in 4 of the pigs were noted at the time of measurement so a second set of data were collected immediately afterward. In another 19 cases, technical problems were not noted at the time of measurement (the oscillator failed to activate, the data collection was mistakenly omitted, or inspiration was not long enough), so these data were discarded, leaving 261 satisfactory data epochs.

Statistics

Expiratory and inspiratory E_2 parameters were analyzed separately using a two-way ANOVA (SigmaPlot version 12, Systat Software, Chicago, IL), with group and time as factors. Post hoc comparisons were made using the Tukey HSD test.

Results

Time-domain analysis

We fit each of the models listed in Table 1 to segments of $\dot{V}$ and P starting at 0.5 s before the beginning of expiration and ending 2 s after the start of the following inspiration. We found that while the models captured the overall nature of the $P(t)$ data, there were clear systematic differences between the data and the model fit in all cases, particularly during expiration. Significantly better fits were obtained when the data segments were divided into their expiratory and inspiratory phases and the models fit to each phase separately. Figure 1 shows the RMSR, AICc, and the Akaike weights for each model separately for expiration and inspiration, as well as for the entire breath. Model 4 provided the best fits in all cases, with overwhelming Akaike weight probabilities that it was the best of the five models (Fig. 1C). Figure 2 shows examples of Model 4 fitted to the whole breath (Fig. 2A), to expiration only (Fig. 2B), and to inspiration only (Fig. 2C).

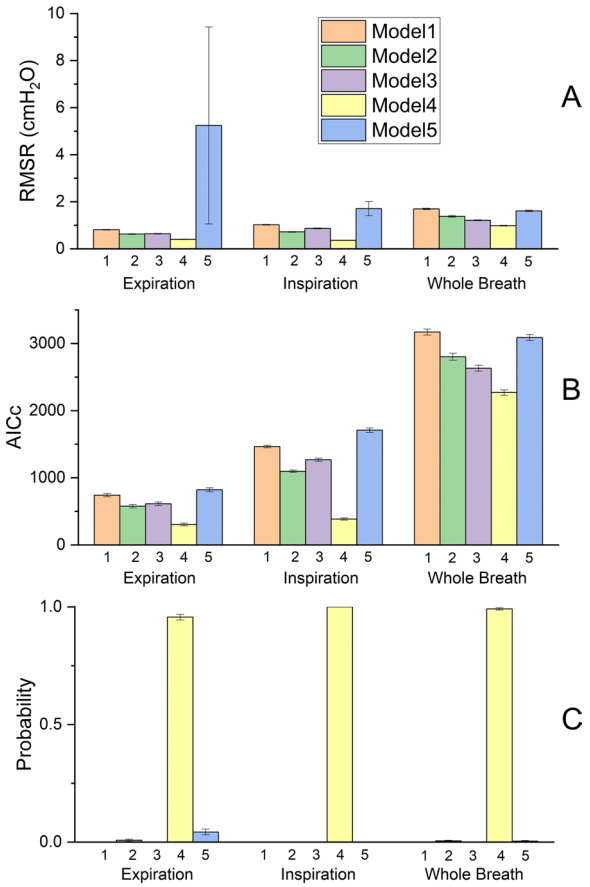

Fig. 1 **A** Root mean squared residual (mean ± SE) for all 5 models in Table 1 for expiration only, inspiration only, and the whole breath. RMSR for Model 5 during expiration appears anomalously large compared to the other values, but this was due to a small number of cases in which the model was extremely poor. **B** Corresponding corrected Akaike criteria (AICc). **C** Probabilities (Akaike weights) that each model is the best for each phase of the breath

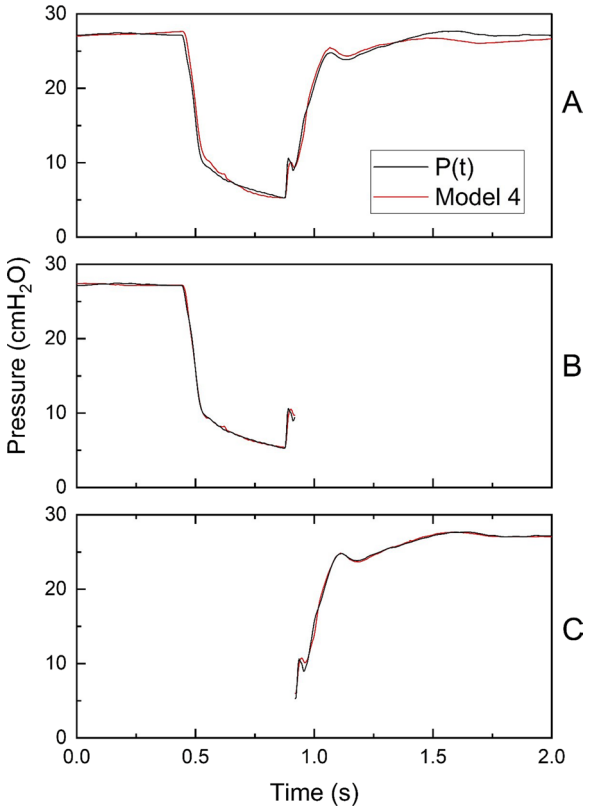

Fig. 2 Example measured $P(t)$ (black line) and the fits provided by Model 4 (red line) for **A** The whole breath, **B** Expiration only, and **C** Inspiration only in a representative pig receiving APRV with $P_{High} = 28$ cmH_2O and expiration terminated at 25% peak expiratory flow

Accordingly, we focus our attention on Model 4, and its elastic behavior specifically, because of the opposing effects of OD and RD; OD is expected to cause lung tissue to become stiffer with increasing V, while recruitment of closed lung units during inspiration is expected to have the opposite effect. The pressure–volume relationship of Model 4 is captured by the values of the parameters E_1 and E_2. However, the value of E_1 is affected by the definition of $V = 0$, which we arbitrarily set as the lung volume at end-expiration. Since end-expiratory lung volume depends on T_{Low} in APRV, comparison of E_1 values across the four study groups is problematic. E_2, on the other hand, is not affected by the designation of $V = 0$ (see Appendix for a mathematical proof). Importantly, E_2 is positive when tissue stiffness increases with V and negative when stiffness decreases with V. Accordingly, it is the parameter E_2 that reveals whether

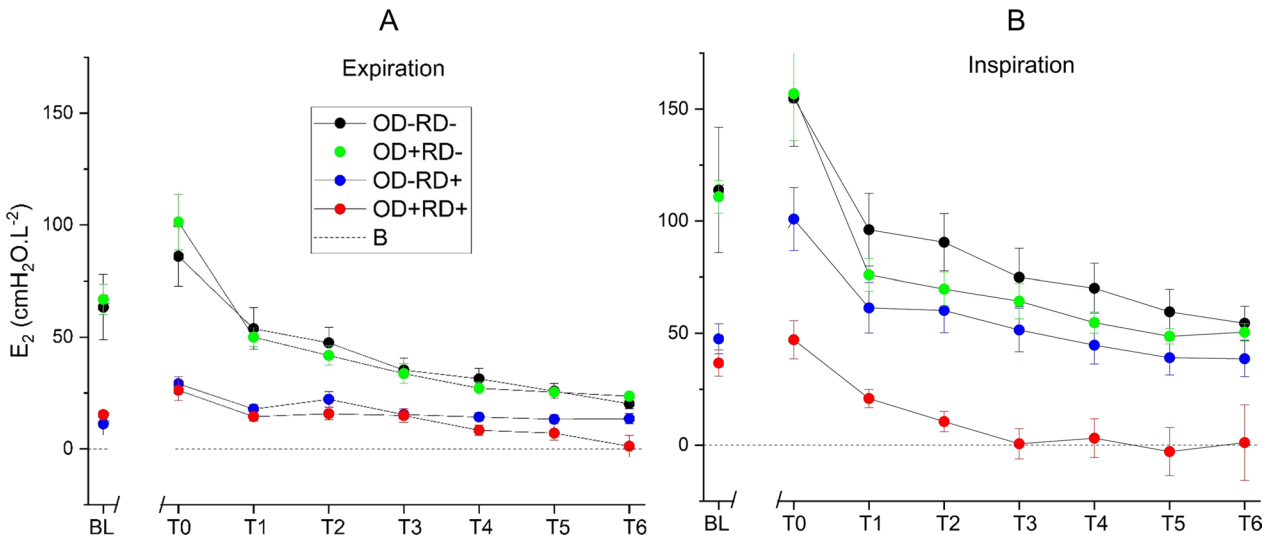

Fig. 3 The parameter E_2 that defines the curvature of the dynamic pressure–volume relationship for each group at each time point for **A** Expiration, and **B** Inspiration. BL represents the baseline measurements. T0 is immediately after lavage injury, while T1 through T6 are at subsequent 1 h intervals

OD dominates over RD (in which case it is positive), or vice versa (in which case it is negative).

Figure 3 shows E_2 for each group at each time point for both the expiratory fits (Fig. 3A) and the inspiratory fits (Fig. 3B) as described below:

Expiration: Visual inspection of the data suggests (Fig. 3A) and statistical analysis confirms that there are no significant differences in E_2 between the two RD- groups (OD−RD− and OD + RD−), and also no significant differences between the two RD + groups (OD−RD + and OD + RD +) at any of the time points (i.e., BL through T6, $p < 0.05$). Thus, within each RD condition (RD + or RD−), OD does not influence E_2. In addition, the RD- groups demonstrate significant time-dependent reductions in E_2 from T0 to T1 ($p < 0.001$). Also, T1 is significantly different from E_2 for T3 and beyond ($p < 0.05$). In contrast, for the OD + RD + group, the time-dependent response occurs over much longer time scales as evident by significant differences in E_2 only between T0 and T4 ($p < 0.05$), T0 and T5 ($p < 0.05$) and T0 to T6 ($p < 0.001$). Finally, for OD−RD +, there is no significant time-dependent change in E_2 over all times. These findings suggest that recovery from injury is minimal in the RD + condition.

Inspiration: Visual inspection of Fig. 3B suggests and statistical analysis confirms that inspiratory E_2 is not significantly different between the two RD− groups (OD−RD− and OD + RD−) at any time point. While there is a significant initial difference (T0) in E_2 between the two RD- groups and OD−RD + ($p < 0.01$), for T1 onwards, those differences are not significant ($p > 0.05$). Most notably, there is a highly statistically significant difference between OD + RD + and all other groups for all time points ($p < 0.001$). Furthermore, $E_2 \sim 0$ from T3 onwards, illustrating that in the OD + RD + condition, tissue stiffness is independent of lung volume as embodied in the parameter E_1. Finally, in all cases, E_2 is significantly greater at T0 compared to all other time points ($p < 0.001$), but this trend continues past T0 only in the OD-RD- group for which E_2 is statistically reduced at T2 versus T1 ($p < 0.05$), and at T6 versus T1 ($p < 0.01$).

Oscillometric impedance analysis

Figure 4A shows the parameter R_{rs} obtained by fitting Eq. 1 to measurements of impedance calculated within a 1-s window that was slid over the first 2 s of inspiration averaged over all time points (BL through T6) for each of the four study groups. Figures 4B and C show corresponding plots of E_{rs} and I_{rs}, respectively. The ± SE ranges about each mean curve reveal those differences across groups that can be considered significant. These differences are most evident for R_{rs} as seen in Fig. 4A, which also shows that the two RD + groups are qualitatively different from the two RD- groups. Specifically, the RD + groups both exhibit a knee in their R_{rs}-time relationships at about 0.5 s; in the case of RD + OD + this knee corresponds to an actual peak in the relationship whereas for RD + OD− it is merely an inflection. By contrast, the two RD- groups exhibit very early peaks in R_{rs} around 0. 1 s, after which they decrease monotonically. E_{rs} and I_{rs} (Figs. 4B and C, respectively)

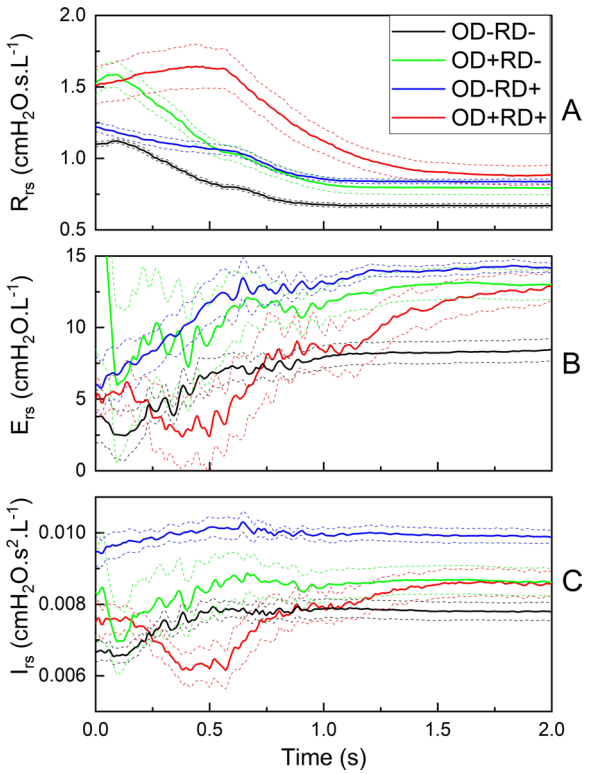

Fig. 4 **A** Resistance, **B** Elastance, and **C** inertance of the respiratory system obtained by fitting the single-compartment model to impedance calculated within a 1-s sliding window over the first 2 s of inspiration for each of the four groups (solid – mean, dashed lines—± standard error)

are considerably noisier than R_{rs}. Also, both E_{rs} and I_{rs} move in the same direction as each other, and opposite to R_{rs} (Fig. 4A). Both E_{rs} and I_{rs} exhibit minima at about 0.5 s for the OD + RD + group, corresponding to the maximum exhibited by R_{rs} for that group.

Discussion

The results of this study, derived from both time-domain and frequency-domain analyses of airway pressure-flow data, indicate that progressive inspiratory lung recruitment occurs during APRV when expiration is terminated at 25%, as opposed to 75%, of peak flow. Our explanation for these findings is that brief expirations do not permit sufficient time for the lung to derecruit during expiration, since both recruitment and derecruitment are known to be dynamic events that take a certain amount of time to manifest when pressure conditions are conducive. We cannot discount the possibility, however, that derecruitment may also have been facilitated by the lower transpulmonary pressures reached during the longer expirations, so there may have been both time and pressure effects involved. Regardless of the relative contributions of time and pressure however, our results provide clear evidence that limiting the duration of expiration reduces expiratory derecruitment and, by implication, the atelectrauma that results from repetitive recruitment during inspiration.

Mortality from ARDS has not decreased significantly in over 20 years, and remains alarmingly high despite the advent of protective low-Vt ventilation following the seminal ARDSnet trial in 2000 [21]. This motivates the ongoing search for improved strategies for mechanically ventilating the injured lung, the preeminent goal being to avoid VILI by attempting to minimize overdistension and/or intra-tidal recruitment. Since 2000, however, the only other strategy shown to reduce ARDS mortality is prone positioning [31]. Neither PEEP titration based on best compliance [8] nor high-frequency oscillatory ventilation [32, 33] have been shown to provide mortality benefits, despite both being based on sound physiologic rationales [34, 35]. The subject of the present study, APRV with a sufficiently small expiratory duration, is also based on a hypothesized rationale, namely avoiding atelectrauma by not giving derecruitment enough time to manifest during expiration [18]. While such a strategy has yet to be subjected to a randomized clinical trial, studies in animal models of lung injury [15, 36, 37] and case studies in human ARDS patients [38] have shown promising results.

The success of APRV in reducing the potential for VILI depends critically on the choice of T_{Low}. We have shown that terminating expiration when the flow has fallen to 75% of its early peak value is protective against VILI [14, 16, 39]. This typically results in $T_{Low} \sim 0.5$ s, but the precise value varies with the injury status of the lung, making the approach both adaptive and personalizable within and across patients. By contrast, allowing expiratory flow to fall to 25% of its peak value has been shown to lead to VILI, even though this translates to a T_{Low} of only about 1.5 s in the Tween model of acute lung injury [17]. This indicates that the margin of error in expiratory duration is about 1 s, which illustrates the practical challenges of implementing this strategy safely. Terminating expiration at 75% of peak flow is a purely empirical strategy, so whether it can be improved upon remains unknown. There is thus a strong need to understand the physiologic basis of using brief expirations so that they can be utilized in an optimal manner.

One of the most notable findings in this study is that during inspiration, E_2 is substantially lower in the OD + RD + group compared to the other three groups (Fig. 3). We have previously shown [4] that this was the only one of the 4 groups not to have recovered to non-ARDS levels of PaO_2:FiO_2 after 6 h of APRV following

Tween lavage injury. The findings of the present study thus imply that the value of E_2 during inspiration contains potentially clinically useful information that could be used to titrate T_{Low} to a longer value (thereby improving CO_2 elimination) while still avoiding atelectrauma. Inspection of Fig. 3B suggests, for example, that inspiratory E_2 should not be allowed to fall below about 50 $cmH_2O.L^{-2}$ for the pigs in our study. The threshold value of E_2 for incurring injury might be different for humans compared to pigs, and it also likely varies with the type and severity of injury [13]. Nevertheless, these results show that evaluation of intra-breath respiratory mechanics may identify a signature of intra-tidal recruitment that can be implemented at the bedside, and which could serve as a biomarker to direct adjustments in T_{Low}.

The lower E_2 values seen in both RD + compared to the two RD− groups (Figs. 3A and 3B, respectively) are likely reflective of lung derecruitment during expiration and re-recruitment during inspiration. That is, the dynamic pressure–volume relationships are less curved in the RD + groups compared to the two RD− groups because ongoing derecruitment (during expiration) and recruitment (during inspiration) offsets the intrinsic strain stiffening behavior of the lung parenchyma. In fact, this is not a new concept; the same idea has been invoked in previous studies of more conventional mechanical ventilation strategies [25–27, 40]. Our physiologic interpretation of E_2 is based, however, on the validity of the choice of model for describing respiratory system mechanics. We investigated five different models (Table 1), each selected given their precedents in the literature as well as the fact that they can be fitted to airway pressure-flow data by multiple linear regression, allowing their parameters to be estimated rapidly and definitively [23, 41]. These models also collectively cover the two canonical possibilities beyond the single-compartment linear model (Model 1), namely nonlinear constitutive properties (Models 2 thru 4) and multi-compartment topology (Model 5). Model 4, with its flow-dependent resistance and volume-dependent elastance, consistently outperformed the other 4 models (Fig. 1), making it the model of choice for determining E_2. However, the fits of all models were not particularly good when applied over the entire APRV breath but were markedly improved when applied to the expiration and inspiration phases separately (Figs. 1 and 2). This indicates that different physiologic phenomena occurred during expiration vs. inspiration that none of the models accounted for. It is likely that such phenomena relate to the dependence of RD on time as well as pressure, and that apparent elastic properties have different dependencies on volume depending on the phase of the respiratory cycle. Indeed, this is precisely why we conjecture that APRV reduces risk for VILI, provided T_{Low} is chosen appropriately [18].

To further investigate differences between expiratory and inspiratory lung mechanics, we tracked time-varying respiratory system impedance using oscillometry. This requires specialized equipment beyond what is normally found in an intensive care unit. Thus, while deployable in principle, oscillometry is less suited for routine monitoring of RD biomarkers in the intensive care unit compared to the time-domain model parameters discussed above. However, oscillometry does provide a more detailed perspective of mechanical events that may evolve within a breath. As with E_2 in Fig. 3, impedance during inspiration exhibits a characteristic behavior in the OD + RD + group that is absent in the other 3 groups, namely a peak at about 0.5 s that is most clearly apparent in resistance (Fig. 4A). The OD−RD + group shows an inflection around the same time point, suggesting that both groups experienced some mechanical transition within half a second into inspiration. This indicates that T_{Low} was long enough in these two groups for derecruitment to have begun before the start of the subsequent inspiration. Once underway, this derecruitment continued on into the early part of inspiration until lung volume increased to the point of starting to reverse it, which in this case occurred at about 0.5 s. The two RD− groups with their shorter T_{Low} also showed peaks in resistance that were much closer to $t = 0$ (Fig. 4A). This is compatible with the idea that RD was less pronounced compared to the two RD + groups. Nevertheless, the fact that the two RD− groups showed any peak at all suggests the possibility that a slightly shorter T_{Low} might have been better in terms of avoiding atelectrauma. Thus, oscillometry could potentially be used to adjust T_{Low} such that this peak in resistance is eliminated.

Differences in the behavior of oscillometric elastance (E_{rs} in Fig. 4B) and inertance (I_{rs} in Fig. 4C) for the OD + RD + group were also apparent, although the signals were considerably noisier compared to R_{rs}. Since E_{rs} and I_{rs} are both derived from the reactive component of impedance, their signal-to-noise ratios over time may be worse than R_{rs}, which is the only parameter derived from the resistive component of impedance. Curiously, E_{rs} and I_{rs} for the OD + RD + group both move in the same direction, which is opposite to that for R_{rs}. This is somewhat curious because I_{rs} is usually thought of as largely reflecting the mass of the gas in the conducting airways, and thus it should increase with increasing airway radius, as does R_{rs}, and vice versa [42]. The pigs in this study, however, had a resonant frequency around 6 Hz, which is somewhat lower than the roughly 10 Hz

found in humans [43]. Since resonant frequency depends on the ratio of E_{rs} to I_{rs} [23], this unexpected finding may indicate that chest wall and lung parenchymal tissue masses may also contribute to I_{rs} in pigs, in which case it could track with E_{rs} which is also a property of the tissues. In any case, the results of the present study would seem to suggest that resistance alone serves as the most useful indicator of RD dynamics throughout inspiration.

Finally, we must acknowledge that although our findings may be taken as reflective of the time dependence of expiratory derecruitment based on experimental [12, 13] and computational [18] evidence, we cannot discount the possibility that transpulmonary pressure also played a role. That is, the longer expiratory durations in the two RD+ groups would have allowed lung volumes (and thus transpulmonary pressures) to descend to lower levels compared to the two RD− groups. This could have allowed more derecruitment to take place purely as a result of the lower levels of intrinsic PEEP in the RD− groups [44]. However, the fact that the knees in the R_{rs} curves from the two RD− groups occur essentially at the beginning of inspiration (Fig. 4A) suggests that there was almost no derecruitment to reverse despite expiration have a duration of approximately 0.5 s. This implies that derecruitment requires a finite duration of time to begin to manifest when pressures are reduced. Regardless of the relative roles of time and pressure, our results provide clear evidence that intra-tidal recruitment and derecruitment is avoided if expirations are sufficiently brief.

Our study has a number of limitations. The Tween lavage injury used here produces a convenient model of surfactant dysfunction, which is a key feature of ARDS, but is arguably less relevant to clinical ARDS than other models, such as direct injury to the epithelium by acid instillation or injury induced by endotoxin. Our inferences about intra-tidal RD are indirect, being based on model analyses of airway pressure-flow relationships. While these inferences are based on accepted physiologic reasoning, they do not constitute objective proof that dynamic RD is responsible for our observations. We investigated a number of different models of lung mechanics to explain the shape of the pressure waveform during expiration and inspiration, but these models are simple in the interests of their parameters being easily calculated and were selected on the basis of a model hierarchy [23]. There may exist alternative, more complex models that account for the data better, and that provide different insights than those we gained in the present study. Similarly, our inferences drawn from impedance measurements during inspiration were based on a temporal resolution of 1 s. A finer resolution might have revealed data features not apparent in the data of the present study. Finally, although our results suggest that threshold behaviors for E_2 and R_{rs} that could serve as physiologic biomarkers to set the value of T_{Low}, a more exhaustive study of these parameters is required before their utility can be maximized.

In conclusion, we have shown that signatures of lung recruitment during inspiration in APRV support the hypothesis that brief expirations are efficacious against atelectrauma because they do not allow sufficient time for expiratory derecruitment to occur. These signatures can be derived, breath-by-breath in real time, from analysis of airway pressure and flow waveforms created either by the ventilator or by an external oscillator. If implemented at the bedside, this information would provide a means for ongoing adjustment of T_{Low} to maintain adequate gas exchange while avoiding the risk of VILI.

Appendix

Analysis of elastic nonlinearities

The equation of Model 4 is

$$P(t) = R_1\dot{V}(t) + R_2\dot{V}(t)\left|\dot{V}(t)\right| + E_1V(t) + E_2V^2(t) + \lambda t + P_0. \tag{2}$$

where R_1, R_2, E_1, E_2, α and P_0 are parameters determined by multiple linear regression. Because we do not have an independent estimate of functional residual capacity, V is expressed relative to an arbitrary baseline that differs from the elastic equilibrium volume of the respiratory system by some amount V_0. Equation 2 is thus re-written as

$$\begin{aligned} P(t) &= R_1\dot{V}(t) + R_2\dot{V}(t)\left|\dot{V}(t)\right| + E_1[V(t)+V_0] \\ &\quad + E_2[V(t)+V_0]^2 + \lambda t \\ &= R_1\dot{V}(t) + R_2\dot{V}(t)\left|\dot{V}(t)\right| + (E_1 + 2E_2V_0)V(t) \\ &\quad + E_2V^2(t) + \left(E_1V_0 + E_2{V_0}^2\right) + \lambda t \\ &= R_1\dot{V}(t) + R_2\dot{V}(t)\left|\dot{V}(t)\right| + AV(t) + BV^2(t) + C + \lambda t. \end{aligned} \tag{3}$$

The parameters R_1, R_2, A, B, C and α are obtained by multiple linear regression, where

$$A = E_1 + 2E_2V_0, \tag{4}$$

$$B = E_2, \tag{5}$$

and

$$C = E_1V_0 + E_2{V_0}^2 = E_1V_0 + B{V_0}^2 \tag{6}$$

From Eqs. 4 and 5,

$$E_1 = A - 2BV_0. \tag{7}$$

Thus, while E_2 is provided directly from Eq. 5, evaluating E_1 requires knowledge of V_0, which can be solved for as follows. Substituting Eq. 7 into Eq. 6 gives

$$C = (A - 2BV_0)V_0 + BV_0^2 \tag{8}$$

which rearranges to give

$$BV_0^2 - AV_0 + C = 0. \tag{9}$$

Therefore,

$$V_0 = \frac{A \pm \sqrt{A^2 - 4BC}}{2B}. \tag{10}$$

Regardless of which root in Eq. 10 is the correct one, the model does not describe real data perfectly and A, B and C are regression parameters that are affected by noise. There is thus no guarantee that the discriminant in the above quadratic solution is positive, and indeed we sometimes found it to be negative in which case the above theory returned a physically meaningless complex value for V_0. This means that E_1 cannot be reliably estimated via Eq. 7 when elastic recoil is represented as a quadratic function of V, and V itself is expressed relative to an arbitrary baseline. By contrast, E_2 is equal to the regression parameter B, and thus is independent of uncertainty in V_0.

Abbreviations

AICc	Corrected Akaike criterion
ANOVA	Analysis of variance
APRV	Airway pressure release ventilation
ARDS	Acute respiratory distress syndrome
EEF	End-expiratory flow
OD (±)	Over-distension (greater or less)
PEEP	Positive end-expiratory pressure
RD (±)	Recruitment and derecruitment (greater or less)
RMSR	Root mean squared residual
VILI	Ventilator-induced lung injury
P_{High}	The high pressure applied during inspiration in APRV
P_{Low}	The low pressure applied during expiration in APRV
T_{High}	The duration of inspiration in APRV
T_{Low}	The duration of expiration in APRV
t	Time
P(t)	Pressure (as a function of time)
$\dot{V}(t)$	Flow (as a function of time)
$V(t)$	Volume (as a function of time)
f	Frequency
$Z(f)$	Impedance (as a function of frequency)
R	Resistance in Model 1
R_1	Flow-independent resistance in Models 2 and 4
R_2	Flow-dependent resistance in Models 2 and 4
E	Elastance in Model 1
E_1	Volume-independent elastance in Models 3 and 4
E_2	Volume-dependent elastance in Models 3 and 4
α	A parameter in Model 5
β	A parameter in Model 5
γ	A parameter in Model 5
δ	A parameter in Model 5
λ	A parameter in Model 5
ρ	A parameter in Model 5
P_0	Baseline pressure (when flow and volume are zero) in Models 1–4
R_{rs}	Respiratory system resistance identified from impedance
E_{rs}	Respiratory system elastance identified from impedance
I_{rs}	Respiratory system inertance identified from impedance

Acknowledgements
The authors acknowledge the help of Nirav Daphtary, M.Sc., who constructed the oscillometry device used to make the impedance measurements reported herein.

Author contributions
JHTB, GFN and DPG conceived and designed the study. MKS and GFN performed the animal experimentation. JHTB analyzed the data and drafted the manuscript. DWK and DPG provided critical input to the data analysis. All authors reviewed and approved the final manuscript.

Funding
This work was supported in part by NIH grant R01HL142702, and by the Office of the Assistant Secretary of Defense for Health Affairs, through the Peer Reviewed Medical Research Program under Award Nos. W81XWH-20-1-0696 and W81XWH-21-1-0507. Opinions, interpretations, conclusions, and recommendations are those of the authors and are not necessarily endorsed by the Department of Defense.

Availability of data and materials
Data are available from the authors on request.

Author details
[1]Department of Medicine, University of Vermont, University of Vermont Larner College of Medicine, 149 Beaumont Avenue, Burlington, VT 05405, USA. [2]Departments of Anesthesia, Biomedical Engineering, and Radiology, University of Iowa, Iowa City, IA 52242, USA. [3]Department of Surgery, SUNY Upstate Medical Center, Syracuse, NY 13210, USA. [4]Department of Biomedical Engineering, Tulane University, New Orleans, LA, USA.

Received: 22 July 2024 Accepted: 29 September 2024
Published online: 08 October 2024

References

1. Gaver DP 3rd, Nieman GF, Gatto LA, Cereda M, Habashi NM, Bates JHT. The POOR get POORer: a Hypothesis for the pathogenesis of ventilator-induced lung injury. Am J Respir Crit Care Med. 2020;202(8):1081–7.
2. Nieman G, Kollisch-Singule M, Ramcharran H, Satalin J, Blair S, Gatto LA, et al. Unshrinking the baby lung to calm the VILI vortex. Crit Care. 2022;26(1):242.
3. Seah AS, Grant KA, Aliyeva M, Allen GB, Bates JH. Quantifying the roles of tidal volume and PEEP in the pathogenesis of ventilator-induced lung injury. Ann Biomed Eng. 2011;39(5):1505–16.
4. Ramcharran H, Bates JHT, Satalin J, Blair S, Andrews PL, Gaver DP, et al. Protective ventilation in a pig model of acute lung injury: timing is as important as pressure. J Appl Physiol. 2022;133(5):1093–105.
5. Tremblay L, Valenza F, Ribeiro SP, Li J, Slutsky AS. Injurious ventilatory strategies increase cytokines and c-fos m-RNA expression in an isolated rat lung model. J Clin Invest. 1997;99(5):944–52.
6. Cipulli F, Vasques F, Duscio E, Romitti F, Quintel M, Gattinoni L. Atelectrauma or volutrauma: the dilemma. J Thorac Dis. 2018;10(3):1258–64.
7. Crotti S, Mascheroni D, Caironi P, Pelosi P, Ronzoni G, Mondino M, et al. Recruitment and derecruitment during acute respiratory failure: a clinical study. Am J Respir Crit Care Med. 2001;164(1):131–40.
8. Sahetya SK, Goligher EC, Brower RG. Fifty years of research in ARDS. Setting positive end-expiratory pressure in acute respiratory distress syndrome. Am J Respir Crit Care Med. 2017;195(11):1429–38.
9. Meade MO, Cook DJ, Guyatt GH, Slutsky AS, Arabi YM, Cooper DJ, et al. Ventilation strategy using low tidal volumes, recruitment maneuvers, and high positive end-expiratory pressure for acute lung injury and acute respiratory distress syndrome: a randomized controlled trial. JAMA. 2008;299(6):637–45.

10. Mercat A, Richard JC, Vielle B, Jaber S, Osman D, Diehl JL, et al. Positive end-expiratory pressure setting in adults with acute lung injury and acute respiratory distress syndrome: a randomized controlled trial. JAMA. 2008;299(6):646–55.
11. Brower RG, Lanken PN, MacIntyre N, Matthay MA, Morris A, Ancukiewicz M, et al. Higher versus lower positive end-expiratory pressures in patients with the acute respiratory distress syndrome. N Engl J Med. 2004;351(4):327–36.
12. Albert SP, DiRocco J, Allen GB, Bates JH, Lafollette R, Kubiak BD, et al. The role of time and pressure on alveolar recruitment. J Appl Physiol. 2009;106(3):757–65.
13. Allen G, Bates JH. Dynamic mechanical consequences of deep inflation in mice depend on type and degree of lung injury. J Appl Physiol. 2004;96(1):293–300.
14. Emr B, Gatto LA, Roy S, Satalin J, Ghosh A, Snyder K, et al. Airway pressure release ventilation prevents ventilator-induced lung injury in normal lungs. JAMA Surg. 2013;148(11):1005–12.
15. Kollisch-Singule M, Emr B, Jain SV, Andrews P, Satalin J, Liu J, et al. The effects of airway pressure release ventilation on respiratory mechanics in extrapulmonary lung injury. Intensive Care Med Exp. 2015;3(1):35.
16. Kollisch-Singule M, Emr B, Smith B, Roy S, Jain S, Satalin J, et al. Mechanical breath profile of airway pressure release ventilation: the effect on alveolar recruitment and microstrain in acute lung injury. JAMA Surg. 2014;149(11):1138–45.
17. Jain SV, Kollisch-Singule M, Satalin J, Searles Q, Dombert L, Abdel-Razek O, et al. The role of high airway pressure and dynamic strain on ventilator-induced lung injury in a heterogeneous acute lung injury model. Intensive Care Med Exp. 2017;5(1):25.
18. Bates JHT, Gaver DP, Habashi NM, Nieman GF. Atelectrauma versus volutrauma: a tale of two time-constants. Crit Care Explor. 2020;2(12): e0299.
19. Percie du Sert N, Ahluwalia A, Alam S, Avey MT, Baker M, Browne WJ, et al. Reporting animal research: explanation and elaboration for the ARRIVE guidelines 20. PLoS Biol. 2020;18(7):3000411.
20. Slutsky AS, Ranieri VM. Ventilator-induced lung injury. N Engl J Med. 2013;369(22):2126–36.
21. Brower RG, Matthay MA, Morris A, Schoenfeld D, Thompson BT, et al. Ventilation with lower tidal volumes as compared with traditional tidal volumes for acute lung injury and the acute respiratory distress syndrome. N Engl J Med. 2000;342(18):1301–8.
22. Habashi NM. Other approaches to open-lung ventilation: airway pressure release ventilation. Crit Care Med. 2005;33(3 Suppl):S228–40.
23. Bates J. Lung mechanics. An inverse modeling approach. Cambridge: Cambridge University Press; 2009.
24. Der RF. Strömungswiderstand in den menschlichen Atemwegen und der Einfluss der unregelmässigen Verzweigung des Bronchialsystems auf den Atmungsverlauf in verschiedenen Lungenbezirken. Pflüger's Arch. 1915;162:225–99.
25. Edibam C, Rutten AJ, Collins DV, Bersten AD. Effect of inspiratory flow pattern and inspiratory to expiratory ratio on nonlinear elastic behavior in patients with acute lung injury. Am J Respir Crit Care Med. 2003;167(5):702–7.
26. Kano S, Lanteri CJ, Duncan AW, Sly PD. Influence of nonlinearities on estimates of respiratory mechanics using multilinear regression analysis. J Appl Physiol. 1994;77(3):1185–97.
27. Carvalho AR, Spieth PM, Pelosi P, Vidal Melo MF, Koch T, Jandre FC, et al. Ability of dynamic airway pressure curve profile and elastance for positive end-expiratory pressure titration. Intensive Care Med. 2008;34(12):2291–9.
28. Sato J, Davey BL, Shardonofsky F, Bates JH. Low-frequency respiratory system resistance in the normal dog during mechanical ventilation. J Appl Physiol. 1991;70(4):1536–43.
29. Wagenmakers EJ, Farrell S. AIC model selection using Akaike weights. Psychon Bull Rev. 2004;11(1):192–6.
30. Kaczka DW, Massa CB, Simon BA. Reliability of estimating stochastic lung tissue heterogeneity from pulmonary impedance spectra: a forward-inverse modeling study. Ann Biomed Eng. 2007;35(10):1722–38.
31. Guerin C, Reignier J, Richard JC, Beuret P, Gacouin A, Boulain T, et al. Prone positioning in severe acute respiratory distress syndrome. N Engl J Med. 2013;368(23):2159–68.
32. Ferguson ND, Cook DJ, Guyatt GH, Mehta S, Hand L, Austin P, et al. High-frequency oscillation in early acute respiratory distress syndrome. N Engl J Med. 2013;368(9):795–805.
33. Young D, Lamb SE, Shah S, MacKenzie I, Tunnicliffe W, Lall R, et al. High-frequency oscillation for acute respiratory distress syndrome. N Engl J Med. 2013;368(9):806–13.
34. Battaglini D, Roca O, Ferrer R. Positive end-expiratory pressure optimization in ARDS: physiological evidence, bedside methods and clinical applications. Intensive Care Med. 2024;50(5):762–5.
35. Kaczka DW. Oscillatory ventilation redux: alternative perspectives on ventilator-induced lung injury in the acute respiratory distress syndrome. Curr Opin Physiol. 2021;21:36–43.
36. Roy S, Habashi N, Sadowitz B, Andrews P, Ge L, Wang G, et al. Early airway pressure release ventilation prevents ARDS-a novel preventive approach to lung injury. Shock. 2013;39(1):28–38.
37. Roy S, Sadowitz B, Andrews P, Gatto LA, Marx W, Ge L, et al. Early stabilizing alveolar ventilation prevents acute respiratory distress syndrome: a novel timing-based ventilatory intervention to avert lung injury. J Trauma Acute Care Surg. 2012;73(2):391–400.
38. Andrews PL, Shiber JR, Jaruga-Killeen E, Roy S, Sadowitz B, O'Toole RV, et al. Early application of airway pressure release ventilation may reduce mortality in high-risk trauma patients: a systematic review of observational trauma ARDS literature. J Trauma Acute Care Surg. 2013;75(4):635–41.
39. Kollisch-Singule M, Jain S, Andrews P, Smith BJ, Hamlington-Smith KL, Roy S, et al. Effect of airway pressure release ventilation on dynamic alveolar heterogeneity. JAMA Surg. 2016;151(1):64–72.
40. D'Antini D, Huhle R, Herrmann J, Sulemanji DS, Oto J, Raimondo P, et al. Respiratory system mechanics during low versus high positive end-expiratory pressure in open abdominal surgery: a substudy of PROVHILO randomized controlled trial. Anesth Analg. 2018;126(1):143–9.
41. Kaczka DW, Barnas GM, Suki B, Lutchen KR. Assessment of time-domain analyses for estimation of low-frequency respiratory mechanical properties and impedance spectra. Ann Biomed Eng. 1995;23(2):135–51.
42. Kaczka DW, Mitzner W, Brown RH. Effects of lung inflation on airway heterogeneity during histaminergic bronchoconstriction. J Appl Physiol. 2013;115(5):626–33.
43. Bates JH, Irvin CG, Farre R, Hantos Z. Oscillation mechanics of the respiratory system. Compr Physiol. 2011;1(3):1233–72.
44. Jonson B, Richard JC, Straus C, Mancebo J, Lemaire F, Brochard L. Pressure-volume curves and compliance in acute lung injury: evidence of recruitment above the lower inflection point. Am J Respir Crit Care Med. 1999;159(4):1172–8.

Publisher's Note